Topology-guided Ablation of Atrial Tachycardia

Robin Van Den Abeele[1], Sander Hendrickx[1], Mattias Duytschaever[2], Nele Vandersickel[1]

[1] Ghent University, Ghent, Belgium
[2] AZ Sint-Jan, Brugge, Belgium

Abstract

Following ablation of atrial tachycardia (AT), the tachycardia circuit may switch to a different driver with a slower cycle length instead of terminating. Our aim is to investigate this phenomenon using principles from topology. We apply the index theorem from topology, which states that the sum of all topological charges (TC) must equal zero. Thus, every clockwise rotation (TC = -1) must be paired with a counterclockwise rotation (TC = +1), though these rotations may not always fully complete. Results: To test this hypothesis, 572 unique simulations were generated on a spherical surface with 2D circular boundaries. Additionally, virtual ablations were performed to identify the ablation line that terminates tachycardia. Finally, 24 clinical ATs were retrospectively analyzed. The index theorem was satisfied in 100% of simulations. Virtual ablation successfully terminated tachycardia when boundaries with opposite TC were interconnected, while incorrect ablation slowed the tachycardia cycle length. All 24 clinical cases confirmed these findings. Conclusion: Reentrant atrial tachycardias are sustained by pairs of counter-rotating patterns, and tachycardia is only terminated when boundaries with opposite TC are connected.

1. Introduction

Atrial tachycardias (ATs) are commonly driven by anatomical reentrant circuits that disrupt the heart‘s natural rhythm[1–3]. Ablation is to this day the most common treatment for terminating this type of arrhythmia. However, in some cases the AT does not terminate, instead switching to a new AT with a slower cycle length[4, 5].

In this translational study, we applied principles from topology to create a cohesive framework for investigation of the index theorem on macro reentrant atrial tachycardia (MRAT). Using a spherical mesh model with 2, 3, or 4 holes, we analyzed how the number and spatial distribution of boundaries affect the activation patterns of loops and the outcomes of acute ablation in 572 in-silico MRATs. Additionally, we retrospectively analyzed a cohort of 24 clinical cases.

To achieve this, we employed our own algorithm (DGM-TOP), based on the index theorem [6–8] and calculates phase indexes/topological charges.

1.1. Index theorem

The theorem states that on a closed surface with a finite number of boundaries, the sum of topological charges (TC), or phase indexes I, must equate to zero, ($\Sigma I = 0$). This topological charge of an area enclosed by a circumference C is computed via a contour integral in counterclockwise (CCW) direction:

$$I = \frac{1}{2\pi} \oint_C \vec{\nabla}\phi \cdot \vec{d\ell} \quad (1)$$

Here, $\vec{\nabla}\phi$ represents the spatial phase gradient, and $\vec{d\ell}$ is tangent to the circumference. In AT scenarios, we interpret this normalized phase $\phi/2\pi$ as the local activation time (LAT), normalized by the tachycardia cycle length (TCL). As such, we can redefine equation 1 as:

$$I = \frac{1}{\text{TCL}} \oint_C \vec{\nabla}\text{LAT} \cdot \vec{d\ell} \quad (2)$$

Since the index theorem states that the sum of all the phase indexes is 0, we can deduce that every rotational pattern should be balanced by a counter-rotation pattern in another part of the substrate. In other words: Rotational activity in MRAT exists in pairs of counter-rotating patterns around anatomical boundaries. Concurrently, Santucci et al. [9] provided empirical support for this concept, further validating its significance.

2. Methods

In this study, both in-silico and clinical macro reentrant atrial tachycardias (MRATs) were analyzed by calculating the phase index around each anatomical boundary. The ablation strategy was then compared to the location of boundaries with a non-zero phase index, referred to as critical boundaries (CB). Boundaries with a phase index of zero were labeled as non-critical boundaries (NCB).

2.1. Simulations

Using OpenCARP[10], an open source cardiac electrophysiology simulator, we created a total of 572 unique in-silico MRAT. For our cell model, we used the ten Tusscher-Panfilov model [11], modifying it by reducing the L-type calcium current ICaL by 70% and increasing the rapid delayed rectifier potassium current IKr by 70%. This modified model was then pre-paced at a 250 ms interval (S1-S1) for a duration of 5 seconds to achieve a steady-state condition. For our substrate, a fixed spherical mesh model with holes was chosen because topologically the atria can be considered closed surfaces with a finite number of areas of non-conductive tissue like valves, veins, isolated regions of scar or isolated lines of block.

To create variety in the simulations, we induced MRAT in 572 spherical meshes with varying number, location and size of holes (2-,3-, to 4-holes). Reentry was induced by means of unidirectional block in different locations. In addition, slow conduction zones were placed to increase variety in the models. Finally, virtual ablation lines were placed to assess their effect on MRAT termination or prolongation.

2.2. Clinical cases

For clinical testing, 24 AT cases were collected. 16 ATs were recorded in the AZ-Sint Jan in Brugge and 8 in the Städische Klinikum in Karlsruhe between November 2015 and February 2023. The TCL ranged from 200 ms to 300 ms. 21 ATs contained 3 boundaries, while 3 ATs had 4 boundaries. All cases were selected, based on following criteria:

- The electroanatomical map was of sufficient quality ($\geq$ 0.005 measurement points/mm^2).
- The official diagnosis of the case was known and confirmed through ablation. Additionally, the sequence of ablation lines with corresponding ablation response was recorded.
- The locations of all anatomical boundaries were known.
- The TCL before and after ablation was known.

For each clinical map, a series of cutouts were made in the mesh to define the edges of the anatomical boundaries, including anatomical structures, scar tissue, lines of block, and noisy edge interpolation.

2.3. Index calculation

In this section, we will detail the algorithm used for computing the index of each boundary, for both simulated and clinical cases.

For practical use, we transformed Equation 2 into a Riemann sum, by dividing the boundary into a series of discrete segments S_i, and summing all LAT differences (ΔLAT) between neighboring sections in the CCW direction.

$$\mathrm{I} = \frac{1}{\mathrm{TCL}} \sum_{S_i} \Delta\mathrm{LAT} \quad (3)$$

To compute this value, all boundary points were identified and extracted. These points were then arranged around the geometric center according to their angular coordinates. The boundary was divided into 12 sections, each covering a 30° angle. Each section (S_i) was assigned a corresponding local activation time (LAT, denoted as LAT_i). Outliers were removed by grouping all mesh points within each section into 20 ms intervals and retaining only the bins that contained at least 25% of the total points. Finally, the median of the remaining points was selected as the representative LAT_i value for each section. As such, we can calculate the LAT differences between neighboring section as follows:

$$\Delta\mathrm{LAT}_i = \mathrm{LAT}_{i+1} - \mathrm{LAT}_i \quad (4)$$

3. Results

3.1. Simulations

A total of 572 unique simulations were performed on a spherical mesh, with 200 simulations using 2 boundaries, 192 using 3 boundaries, and 180 using 4 boundaries, resulting in a total of 1,696 boundaries. When calculating the phase index for each boundary, 572 boundaries had an index of +1, 572 had an index of -1, and the remaining 552 boundaries exhibited an index of 0.

Further visual inspection of all boundaries revealed three distinct patterns associated with their expressed phase index: complete rotation, near-complete rotation and parallel activation. These patterns are displayed in Figure 1.

On each of the simulated MRAT, we performed ablation between each boundary pair as illustrated by the example in Figure 2. In 100 % of cases only 1 ablation line was found to terminate the AT, being the line between boundaries of opposite phase index. If any CB is not connected to the other CB with opposite phase index, the AT persisted.

3.2. Clinical data

A total of 24 clinical AT cases were analyzed in depth using our algorithm. Among these, 21 ATs had 3 boundaries, while the remaining 3 ATs had 4 boundaries, resulting in a total of 75 boundaries. After identifying the boundaries, the topological charge (index) was calculated using the DGM-TOP algorithm. In each AT, 2 critical boundaries (CBs) were identified, for a total of 48 CBs.

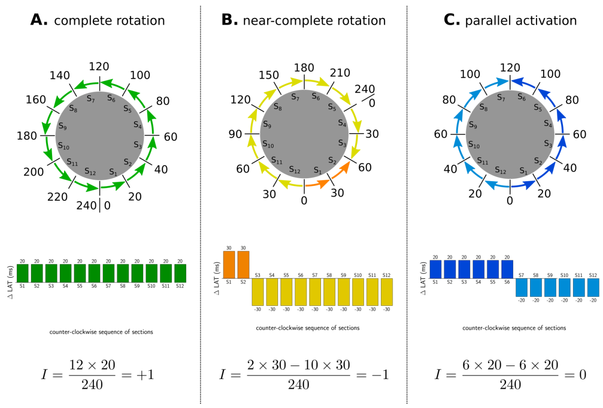

Figure 1. Example of in-silico MRAT with TCL 240 ms with 3 possible patterns around the boundary: **A.** complete rotation **B.** near-complete rotation **C.** parallel activation. Underneath each pattern, you can find the calculation of the phase index and an illustrated via a bar chart.

24 boundaries exhibited an index of +1, while the other 24 exhibited an index of -1. The remaining 27 boundaries were classified as non-critical boundaries (NCBs), having an index of 0. As predicted by the index theorem, the total index in each map was 0. An example is shown in Figure 3

In 16 cases, ablation resulted in termination of the arrhythmia and restoration of sinus rhythm. In these instances, the ablation line successfully interconnected both CBs. However, in the remaining 8 cases, the initial ablation line did not terminate the AT. The DGM-TOP analysis revealed that this ablation line consistently connected a CB to an NCB, allowing the second CB to persist as the primary driver of a new arrhythmia.

For example in Figure 3, the ablation line was placed between the left pulmonary vein (LPV) and the right pulmonary vein (RPV). According to DGM-TOP, this line connected a NCB to a CB, leaving the second CB at the mitral valve (MV) to sustain the new AT.

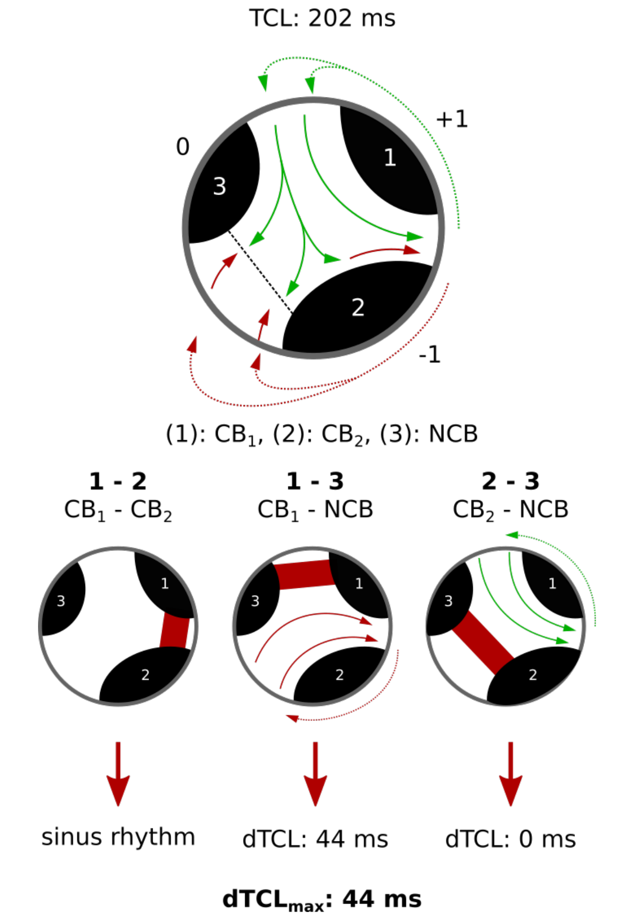

Figure 2. Example of ablation response in a simulated MRAT with TCL of 202 ms. Boundary 1 was found to contain a complete rotation (green circuit), Boundary 2 exhibited a near-complete rotation (red circuit) and boundary 3 parallel activation (Figure 1). Ablation (red line) between boundary 1 and 2 (left panel) was found to terminate the AT and restore sinus rhythm. Ablation between boundary 1 and 3, connects the complete rotation (CB) to the parallel activation (NCB), leaving the near-complete rotation to develop into a complete rotation.

4. Discussion

The index theorem[6, 7] has been proven to be a powerful principle for analyzing mechanisms of MRAT. Through this axiom, we have shown with simulations that critical boundaries exist in pairs around which electrical waves rotate in opposite direction to one another. Additionally, we see that ablation by interconnecting both CBs is the only viable strategy for terminating MRAT. All results are strengthened by a cohort of 24 clinical cases.

In this research, we show a new method DGM-TOP, capable of detecting all critical boundaries. Though this algorithm, we are able to show the clinicians the most effective approach of treating the AT, while also minimizing the ablated surface and thus the damage to the heart, which is critical for maintaining proper heart function. Additionally, preventing wrong ablations will in turn prevent the remapping of patients[4, 5] and therefore speed up the procedure.

This same theory can be applied to other arrhythmias as well, such as bi-atrial tachycardia, atrial fibrillation, ventricular tachycardia and ventricular fibrillation. However, extensive prior testing is needed.

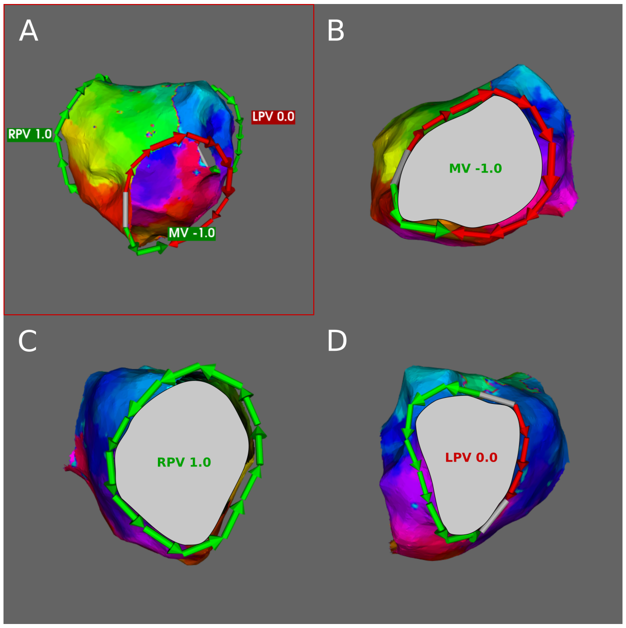

Figure 3. **(A)** Electroanatomical map of AT_1 in anterior-posterior (AP) view. The cyclical colors on the figure represent the LAT of the map. The boundaries are colored in white. **(B)** Conduction around the MV. The index was determined to be -1 **(C)** Conduction around the RPV. The index was calculated to be +1 **(D)** Conduction around the LPV. The index was determined to be 0.

5. Acknowledgements

This research was supported by a 'Starting Grant' from the European Research Council (ERC) under the European Union's Horizon 2020 research and innovation program (Grant No. 900008), awarded to Nele Vandersickel.

References

[1] Markowitz SM, Thomas G, Liu CF, Cheung JW, Ip JE, Lerman BB. Atrial tachycardias and atypical atrial flutters: Mechanisms and approaches to ablation. Arrhythmia Electrophysiology Review 2019;8:131 – 137.

[2] Kuroda S, Wazni OM, Saliba WI, Hilow H, Baranowski B, Tarakji KG, Higuchi K, Tchou P, Dresing T, Lopez JO, et al. The utility of a novel mapping algorithm utilizing vectors and global pattern of propagation for scar-related atrial tachycardias. Journal of Cardiovascular Electrophysiology 2021;32(7):1909–1917.

[3] Vlachos K, Efremidis M, Derval N, Martin CA, Takigawa M, Bazoukis G, Frontera A, Gkalapis C, Duchâteau J, Nakashima T, Letsas KP, Mililis P, Pambrun T, Bourier F, Andre C, Krisai P, Ramirez FD, Kamakura T, Takagi T, Nakatani Y, Kitamura T, Cheniti G, Sacher F, Hocini M, Haïssaguerre M, Jaïs P. Use of high-density activation and voltage mapping in combination with entrainment to delineate gap-related atrial tachycardias post atrial fibrillation ablation. Europace European pacing arrhythmias and cardiac electrophysiology journal of the working groups on cardiac pacing arrhythmias and cardiac cellular electrophysiology of the European Society of Cardiology 2021;.

[4] Arantes L, Klein GJ, Jaïs P, LIM KT, Matsuo S, Knecht S, Hocini M, O'NEILL MD, Clémenty J, Haïssaguerre M. Tachycardia transition during ablation of persistent atrial fibrillation. Journal of cardiovascular electrophysiology 2011;22(5):506–512.

[5] Rostock T, Drewitz I, Steven D, Hoffmann BA, Salukhe TV, Bock K, Servatius H, Aydin MA, Meinertz T, Willems S. Characterization, mapping, and catheter ablation of recurrent atrial tachycardias after stepwise ablation of long-lasting persistent atrial fibrillation. Circulation Arrhythmia and Electrophysiology 2010;3(2):160–169.

[6] Winfree AT, Tyson JJ. When time breaks down: The three-dimensional dynamics of electrochemical waves and cardiac arrhythmias. Physics Today 1988;41(12):107.

[7] Davidsen J, Glass L, Kapral R. Topological constraints on spiral wave dynamics in spherical geometries with inhomogeneous excitability. Physical Review E 2004; 70(5):056203.

[8] Mermin ND. The topological theory of defects in ordered media. Rev Mod Phys Jul 1979;51:591–648.

[9] Santucci PA, Bhirud A, Vasaiwala SC, Wilber DJ, Green A. Identification of 2 distinct boundaries distinguishes critical from noncritical isthmuses in ablating atypical atrial flutter. JACC Clinical Electrophysiology 2023;.

[10] Plank G, Loewe A, Neic A, Augustin C, Huang YL, Gsell MA, Karabelas E, Nothstein M, Prassl AJ, Sánchez J, Seemann G, Vigmond EJ. The opencarp simulation environment for cardiac electrophysiology. Computer Methods and Programs in Biomedicine 2021;208:106223. ISSN 0169-2607.

[11] ten Tusscher KHWJ, Panfilov AV. Alternans and spiral breakup in a human ventricular tissue model. Am J Physiol Heart Circ Physiol Sep 2006;291(3):H1088–H1100.

Address for correspondence:

Robin Van Den Abeele
Proeftuinstraat, 86
9000, Gent
Belgium
robin.vandenabeele@ugent.be